



Revisiting diesel fuel formulation from Petroleum light and middle refinery streams based on optimized engine behavior

Arij Ben Amara, Roland Dauphin, Hassan Babiker, Yoann Viollet, Junseok Chang, Nicolas Jeuland, Amer Amer

► To cite this version:

Arij Ben Amara, Roland Dauphin, Hassan Babiker, Yoann Viollet, Junseok Chang, et al.. Revisiting diesel fuel formulation from Petroleum light and middle refinery streams based on optimized engine behavior. *Fuel*, 2016, 174, pp.63-75. 10.1016/j.fuel.2016.01.062 . hal-01293384

HAL Id: hal-01293384

<https://hal.science/hal-01293384>

Submitted on 24 Mar 2016

HAL is a multi-disciplinary open access archive for the deposit and dissemination of scientific research documents, whether they are published or not. The documents may come from teaching and research institutions in France or abroad, or from public or private research centers.

L'archive ouverte pluridisciplinaire **HAL**, est destinée au dépôt et à la diffusion de documents scientifiques de niveau recherche, publiés ou non, émanant des établissements d'enseignement et de recherche français ou étrangers, des laboratoires publics ou privés.

Revisiting diesel fuel formulation from Petroleum light and middle refinery streams based on optimized engine behavior

Arij Ben Amara¹, Roland Dauphin¹, Hassan Babiker², Yoann Viollet², Junseok Chang², Nicolas Jeuland^{1,3}, Amer Amer²

¹ IFP Energies Nouvelles, 1-4 avenue de Bois-Préau 92852 Rueil-Malmaison Cedex, France

² Saudi Aramco, R&D Center, PO Box 62, Dhahran 31311, Saudi Arabia

³ Present address: Safran Tech, Paris-Saclay, France

* Corresponding author

Contact: arij.ben-amara@ifpen.fr

Abstract

The share of diesel fuel in European transport sector, which currently represents over 50% of total demand, is increasing, requiring massive imports of this product, while at the same time, gasoline fuels are today in surplus. In terms of air pollutant emissions, gasoline and kerosene streams have shown potential in achieving lower emissions in Compression Ignition (CI) engines, particularly nitrogen oxides (NO_x) and particulates. A new fuel formulation approach through the use of light fractions within diesel technology could consequently address both questions of energy demand balance and reduction of diesel engines pollution footprint. In this study, a fuel formulation for a Diesel engine is optimized to achieve lower pollutants emissions and higher engine efficiency. The fuel matrix is based on seven refinery streams representative of gasoline (Hydrotreated Straight-Run Gasoline HSRG, Hydrotreated Fluid Catalytic Cracking HFCC and Reformate REF), kerosene (Hydrotreated Straight-Run Kerosene HSRK and Hydrocracked Kerosene HCKK) and diesel cuts (Hydrotreated Straight-Run Diesel HSRD and Hydrocracked Light Diesel HCKLD). A D-Optimal mixture design is applied to build, a 12-run, 7-factor

fuel matrix and the fuels are thoroughly optimized on two engine conditions at light and mid-load representative of typical vehicle running conditions. The results show a high sensitivity and a good correlation of the engine efficiency and pollutants emissions with the volumetric contribution of each refinery stream to the fuel composition. The optimum fuel composition varies across the range of engine operating points. At light load for example, the addition of up to 50%v of gasoline streams (HSRG and HFCC) to diesel streams demonstrates a good potential to simultaneously reduce NO_x and particulate emissions and an overall good engine performance. Reformate, a highly aromatic gasoline stream, did not offer an advantage at any of the tested conditions due to high particulate emissions. The two kerosene streams perform similarly to diesel streams in terms of engine efficiency and pollutants emissions. A compromise fuel, composed of 50%v HSRG and 50%v HSRD, is proposed that allowed halving NO_x and particulate emissions and reducing the fuel consumption by 5%wt compared to reference diesel HSRD. The optimized fuel represents an alternative for balancing diesel and gasoline demand and for pollutant emissions reduction.

Keywords

Naphtha, Straight-Run Gasoline, Design of Experiment DoE, formulation, optimization, pollutants, efficiency, NO_x, particulates.

1 Introduction

Energy and environmental concerns are driving several changes in the European transport sector, with increasing incentives towards alternative renewable energy sources and new refining processes. However, conventional fossil fuels remain the sector's major energy source. Conventional liquid fuels represented 95% of European demand in 2012 [1] and according to recent forecasts from the European Commission, are likely to remain dominant over the coming decades [2]. For transport applications, the share of diesel fuel represents over 50% of the European market (in comparison with gasoline and jet fuel, 32% and 14% respectively) and demand is rising [2]. The main drivers for such high demand are the high efficiency of diesel engines and recent improvements of after-treatment systems, noise and drivability. Conversely, light products like gasoline cuts, issuing from straight run distillation or Fluid Catalytic Cracking (FCC), a conversion process widely used in European refineries, are today in surplus. This has drawn much attention to their use as an alternative fuel in diesel engines to balance the energy demand and to meet future pollutant emissions legislation. To achieve pollutant targets for light duty diesel engines, several technological solutions are used to enhance the control of ignition timing and combustion rate [3] including variable compression ratio, adapted injection systems, improved piston geometry, increased exhaust gas recirculation (EGR) rates, and improved cooling or boosting capacity [4],[5],[6],[7]. However, the physical and chemical characteristics of a fuel can have an important impact on mixture formation, ignition and heat release rate [8],[9]. Higher volatility enhances the mixture formation during the ignition delay and a lower cetane number delays the ignition occurrence, mainly at low-to-mid loads [10]. Increasing fuel volatility in fuels of similar chemical composition has shown a soot reduction potential in CI engines for diesel and kerosene cuts due to the reduction of over-rich areas, and a moderate effect for gasoline cuts [11]. Increasing diesel volatility at equal cetane number [12] leads to a reduction of liquid film formation on cylinder walls, and thus, a reduction in smoke and enhanced fuel-conversion efficiency. The application of highly mixed combustion modes however presents the disadvantage of a load range limited by difficult combustion control at high load and an increase in HC and CO due to lower

combustion efficiency [7]. Fuel wall impingement, the crevices, boundary layers, and fuel-lean regions formed during longer auto-ignition delay may constitute additional sources of HC and CO emissions [13], [14], [15].

Petroleum-based formulations for Diesel engines and impacts on pollutants

The use of gasoline or kerosene as alternatives to diesel fuel has been studied by several groups for their pollutants reducing potential. Han et al. [16] proved a simultaneous reduction of NO_x and soot emissions using up to 40% gasoline with low EGR requirement compared to diesel fuel. CO and HC emissions were comparable to diesel engines at light loads, however increased at high loads [17]. Kerosene fuels are also attractive for their higher volatility and lower cetane number, generally between EU diesel and gasoline. Tested alone in compression ignition engines, kerosene presents lower NO_x emissions than diesel at a similar soot level [18] [19] and in mixture with diesel, it enhances the combustion efficiency [20]. The chemical effect of fuel formulation is difficult to separate from the physical effect, especially in complex engine configurations. Nevertheless, several general trends have been put forward in recent literature. Most usually, fuels containing high level of aromatics increase soot formation [10] [21]. Diminishing the aromatic content generally correlates with particulate reduction for diesel, gasoline and kerosene distillation cuts [11]. Paraffinic saturated fuels have, in comparison, lower soot tendency regardless of their molecular structure [22] [23]. Note however, the exception of fuels containing a high proportion of long-chain normal paraffins, which may lead to enhanced soot formation through increasing fuel ignitability and the creation of local rich areas [21]. Unsaturated hydrocarbons, namely, monoaromatics and short-chain olefins, can lead to over 2 and 5 folds higher NO_x tendency respectively when compared to paraffinic saturated compounds [24]. Aromatic-rich fuels can have longer ignition delay times but can also form higher level of NO_x towards the end of the combustion [25]. The safety question related to lighter fractions introduction in Diesel fuels has been recently addressed by Al-Abdullah et al. [26] where the flash points (FP) and volatilities of blends of a commercial diesel and a commercial gasoline were measured. According to their results, the flash point decreases as the concentration of gasoline is

increased. For a mixture of 16%vol of gasoline in diesel, FP reaches 40°C. These results suggest that blends with high gasoline fractions should present very similar behavior compared with gasoline which has a FP of 45°C.

Modeling approaches for fuel design

Optimizing a fuel's formulation for advanced combustion modes requires an accurate knowledge of the fuel's behavior over a wide range of engine operating conditions, both in steady state and transient modes. To better address these complex physical and chemical phenomena involved, statistical modeling approaches can represent powerful tools. Especially, Design of Experiments (DoE), refers to the process of planning, designing and analyzing the experiments. It involves the development of statistical relations between the response variables and the input factors and their interactions. In engine applications, DoE have been widely applied in engine optimization processes [27]. DoE has also been used to optimize fuel properties in terms of cetane number (CN), volatility and total aromatics content [28]. However, to our knowledge, few studies have used DoE to optimize the fuel formulation with regards to combustion behavior. In this study, we propose to evaluate a DoE approach to optimize fuel formulation for diesel engines based on existing refinery streams, to improve engine efficiency and reduce main pollutant emissions. Engine outputs were modeled as a function of the fuel composition and an optimum fuel is proposed.

2. Materials and methods

Figure 1 presents the layout of the present study: first, seven refinery streams used in road and air transport were selected. A 12-run, 7-factor D-Optimal mixture design was then generated using Design-Expert® version 9. The seven refinery streams constitute the design variables while engine outputs correspond to the response parameters. Engine outputs were then modeled by first order models with regards to the volume fraction of the streams and the models presenting good quality were used to determine an optimum fuel composition.

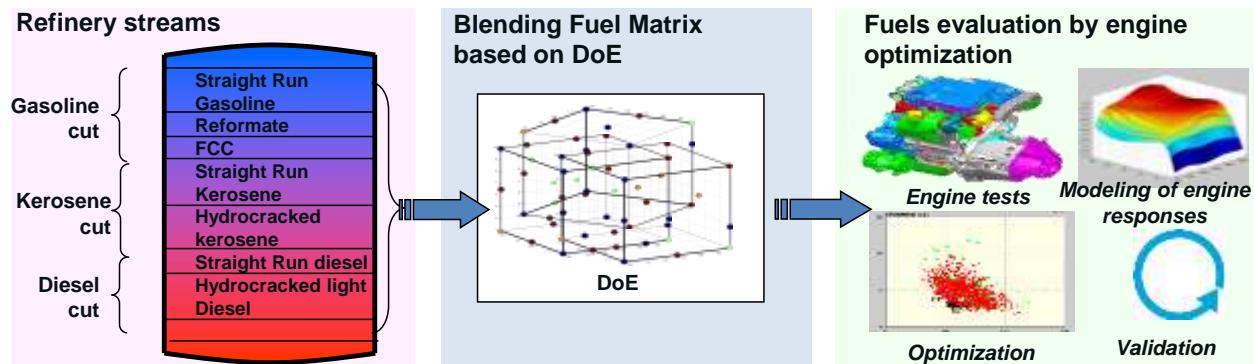


Figure 1: Scheme of the study outline

2.1 Refinery streams

Seven refinery streams representative of gasoline, kerosene and diesel cuts were selected involving three straight-run streams: Hydrotreated Straight Run Gasoline, Kerosene and Diesel, noted, HSRG, HSRK, HSRD, respectively. Main streams properties are presented in Figure 2. Hydrocracked kerosene (HCKK) and light diesel (HCKLD), Hydrotreated Fluid Catalytic Cracking (HFCC) chosen for its high olefins content (near 45%wt) and reformate (REF) constituted of over 97%wt aromatics were selected as the remaining four streams. REF and HSRD were supplied by Coryton Advanced Fuels, and the remaining streams were provided by various Saudi Arabian refineries. All streams have a sulfur content below 10 ppm, except for HSRK which contains 220 ppm (the detailed composition of sulfur containing species were not determined during this work), and they cover a broad distillation range from 35°C to 380°C. Initial Boiling Points vary from 35°C to 188°C and Final Points from 115°C to 380°C. Stream densities vary from 692 to 868 kg/m³ and kinematic viscosity from 0.36 to 3.3mm²/s. Gasoline and kerosene streams have lower values of density and viscosity compared to diesel streams. Paraffins-Olefins-Naphthenes-Aromatics (PONA) composition was determined by gas chromatography mass spectrometry GC-MS analysis and the most paraffinic fuels are the HSRG and HSRK, while naphthenes are the highest in hydrocracked streams (up to 40%wt). REF is composed of over 97%wt aromatics mainly branched monoaromatics (toluene and xylenes), followed by HSRD (45%wt) which has the highest yield of polyaromatics (3.6%wt). Olefins are present exclusively in HFCC at 45%wt. The cetane number was

assessed by CFR technique except for REF and HFCC whose cetane was evaluated by a blending method.

The CN of the streams ranges from 6 to 55. Detailed analysis of the streams is provided in Appendix A.

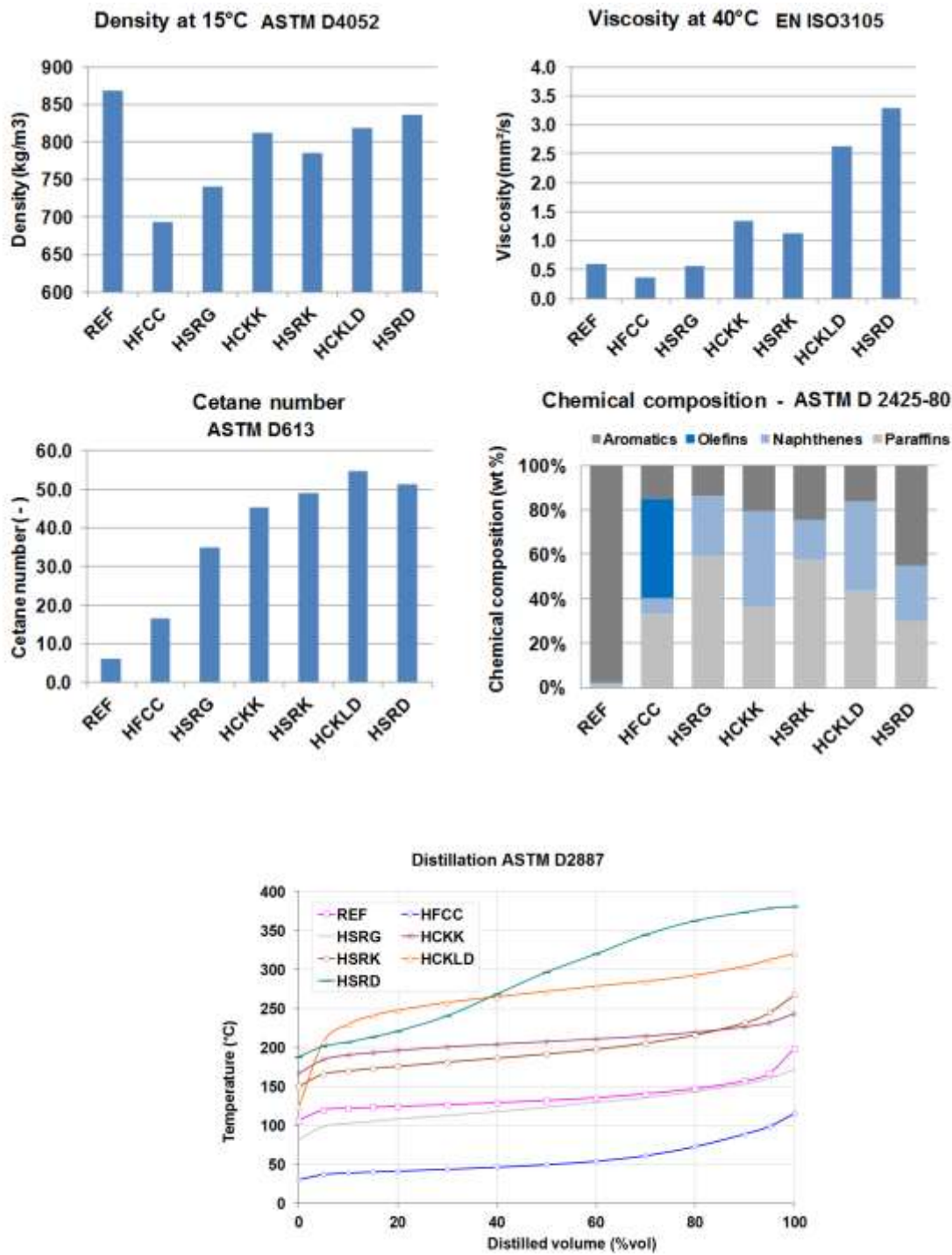


Figure 2: Main fuel properties of the seven selected refinery streams

2.2 Fuel matrix definition by Design of Experiment approach

To optimize fuel composition, a 12-run, 7-factor D-Optimal mixture design was generated using Design-Expert® version 9 [29]. The seven refinery streams constituted the design variables while the engine outputs corresponded to the response parameters. Statistical first-order linear models with no interaction were defined and the matrix was built under constraints of the domain limits. Those limits consisted of the range of cetane number, fractions of diesel, gasoline and kerosene cuts and maximum total aromatics. Hence, the CN range was defined from 35 to 51 (+/-2). The upper limit corresponds to current European diesel specification, and the lower was set to reduce the risk of combustion instability at light load based on previous studies from our group [5]. The proportion of gasoline and kerosene streams was allowed up to 50%vol for each [11] [17] [16] [30], and a minimum of 30%vol of diesel streams was required to allow for high load performance and a sufficient viscosity [5]. In addition, total aromatic content was capped at 50% to limit smoke emissions. The matrix design was composed of 12 (Fuels 1-12) ranked in order of decreasing cetane number. These fuels included a reference diesel fuel (Fuel 4), binary blends of diesel/kerosene streams (Fuel 1 and 2), binary blends of diesel/gasoline streams: Fuels 3 and 12 containing 7%vol and 41%vol Reformate, Fuels 5 and 6 containing 50%vol HSRG and Fuels 10-11 containing 50% HFCC. Two ternary blends of diesel/kerosene/gasoline streams (Fuels 8-9) and a central point (Fuel 7) composed of all tested streams was set as repeatability point and tested 8 times throughout the study (Table 1). Finally, a validation fuel was also formulated (Fuel 13) composed of 50%HCKK, 30%HSRD and 20%HSRG. The matrix is detailed in Table 1. The fuels' properties cover a wide range of physical and chemical properties, some of which were outside the limits of European diesel fuel specifications EN590, especially in terms of density and viscosity. The fuels were treated with lubricity additive (OLI9000 from Innospec) and antioxidant additive (Butylated HydroxyToluene - BHT) to ensure mechanical component durability and a consistent fuel quality throughout the study.

167 *Table 1: Fuel matrix: Fuel 1-12, Fuel 7 corresponds to the central fuel and was tested 8 times throughout*
168 *the study, Fuel 13 is the validation fuel (used for models validation)*

		Unit	Fuel 1	Fuel 2	Fuel 3	Fuel 4	Fuel 5	Fuel 6	Fuel 7	Fuel 8	Fuel 9	Fuel 10	Fuel 11	Fuel 12	Fuel 13
Stream composition	HSRG	%vol	0.0	0.0	0.0	0.0	50.0	50.0	9.7	0.0	0.0	0.0	0.0	0.0	20.0
	HFCC	%vol	0.0	1.7	0.0	0.0	0.0	0.0	11.6	0.0	0.0	46.9	50.0	0.0	0.0
	REF	%vol	0.0	0.0	7.4	0.0	0.0	0.0	11.3	20.0	20.0	0.0	0.0	40.8	0.0
	HSRK	%vol	0.0	50.0	0.0	0.0	0.0	0.0	13.4	50.0	0.0	0.0	0.0	0.0	0.0
	HCKK	%vol	50.0	0.0	0.0	0.0	0.0	0.0	11.9	0.0	50.0	0.0	0.0	0.0	50.0
	HSRD	%vol	0.0	0.0	0.0	100.0	0.0	50.0	19.8	30.0	30.0	53.1	0.0	0.0	30.0
	HCKLD	%vol	50.0	48.3	92.6	0.0	50.0	0.0	22.3	0.0	0.0	0.0	50.0	59.2	0.0
Analyses	Method	Unit													
Density at 15°C	ASTM D4052	kg/m ³	815.6	801.5	822	836.6	781.4	790.7	802.3	817.4	829.8	777.1	763.1	837.2	806
Kin.viscosity 40°C	EN ISO3105	mm ² /s	1.85	1.55	2.11	3.297	1.12	1.21	0.99	1.31	1.36	0.68	0.69	1.33	1.33
Sulfur	EN ISO 20846	mg/kg	1	111	1	2	1	1	31	111	1	3	3	1	1
LHV	ASTM D240	MJ/kg	42.97	43.29	43.13	41.83	41.22	42.79	42.12	42.29	42.65	40.12	40.20	41.95	42.67
CN (CFR)	ASTM D613	-	52.0	51.6	51.6	51.2	46.1	46.1	41.4	41.1	40.0	38.8	36.7	35.2	47.7
H/C/N/O															
C		%wt	86.08	85.90	86.32	86.25	85.68	85.81	86.48	86.89	87.07	86.08	85.94	87.84	86.04
H		%wt	13.76	13.95	13.47	13.75	14.21	14.19	13.44	13.06	12.88	13.91	13.95	12.02	13.91
N		%wt	0.06	0.10	0.11	0.00	0.06	0.00	0.04	0.05	0.00	0.00	0.06	0.07	0.00
O		%wt	0.11	0.05	0.10	0.00	0.06	0.00	0.04	0.00	0.06	0.00	0.06	0.07	0.06
H/C		%wt	1.92	1.95	1.87	1.91	1.99	1.98	1.87	1.80	1.77	1.94	1.95	1.64	1.94
Composition	GCxGC														
Paraffins		%wt	39.9	50.0	40.2	29.9	50.8	43.6	36.9	37.1	27.2	31.3	38.7	26.0	38.5
Naphtenes		%wt	41.6	29.0	37.1	24.6	34.0	25.8	25.0	16.5	28.5	17.2	25.0	23.3	34.4
Olefins		%wt	0.0	0.7	0.0	0.0	0.0	0.0	4.5	0.0	0.0	19.0	20.6	0.1	0.0
Monoaromatics		%wt	17.1	18.9	21.1	41.7	14.3	28.7	32.0	44.5	42.4	30.5	14.8	49.4	25.4
Polyaromatics		%wt	1.5	1.3	1.6	3.6	0.9	1.8	1.5	1.7	1.8	1.9	0.9	1.3	1.7
Total Aromatics		%wt	18.5	20.3	22.7	45.3	15.2	30.5	33.5	46.3	44.2	32.4	15.7	50.7	27.1
Distillation	ASTM D2887														
IBP		°C	161	36	129	202	99	98	36	130	130	36	36	125	98
T50		°C	233	231	267	292	190	197	201	197	205	197	201	212	208
T95		°C	306	326	314	380	306	375	382	369	369	401	328	307	353

169 Figure 3 illustrates the density, viscosity, cetane number and PONA composition of the fuels in the matrix.

170 Diesel-rich and reformate-rich fuels (Fuel 3, 4, 8, 9 and 12) have the higher density, while the lowest

density ones have higher fraction of HSRG and HFCC gasoline streams. Several matrix fuels are under the range of the European specification EN590 (820-845 g/L). Due to the high volatility of several fuels, viscosity could not be measured in the standard 40°C temperature. Pedersen model [31] (validated at 10°C with a correlation coefficient of 0.93) was used to estimate viscosity at 40°C. Calculated viscosity at 40°C is significantly low for the entire matrix compared with European specification EN 590, except for diesel-rich fuels.

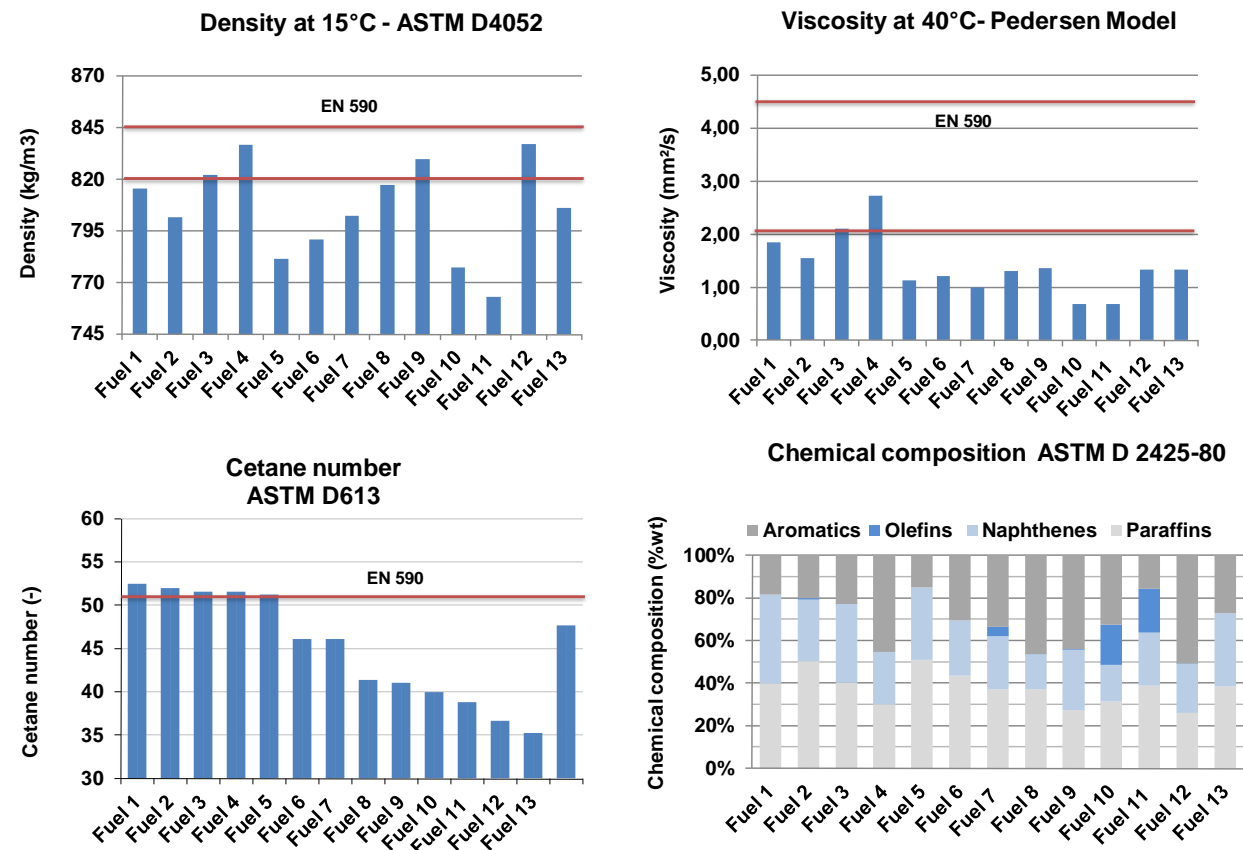


Figure 3: Density, Viscosity at 40°C (Pedersen model), cetane number and chemical composition of the fuel matrix Fuels 1-12 and the validation fuel (Fuel 13)

PONA composition of the matrix fuels was calculated by linear correlation from the data of single streams (Appendix A). Paraffinic compounds (linear and branched) vary from 26 to 51%wt. Aromatics range from 15 to 51%wt. Olefins are present in HFCC containing fuels: i.e. Fuels 2, 7, 10 and 11. They range from 2 to 21%wt. Finally, naphthenes range from 16 to 42%wt. Volatility is the highest for Fuels 2, 10 and 11,

due to HFCC presence even at very low ratio, and Fuels 3 and 5 most likely due to the presence of HCKLD whose IBP is close to gasoline streams.

2.3 Fuel optimization procedure

The experiments were conducted in a DV6D 4-cylinder light duty diesel engine from PSA Peugeot Citroën (PSA), compliant with Euro 5 specification. The engine details are given in Table 2. The engine oil and water temperatures were set to 90°C during the experiment. The engine was equipped with a Bosch CRI2.2 common rail direct fuel injection with a maximum rail pressure of 1800 bar, a turbocharger with a fixed geometry and a high pressure EGR system. The engine was tested without the after-treatment system fitted and an open Engine Control Unit (ECU) was used to monitor injection parameters and air/EGR settings.

Table 2: Details of the DV6D 4-cylinder engine model from PSA

Engine specifications	Value
Bore	75 mm
Stroke	88,3 mm
Displacement	1560 cm ³
Connecting rod length	136,8 mm
Compression ratio	16:1
Intake valve opening	377 °CA
Intake valve closing	550 °CA
Intake valve maximum lift	9,25 mm
Exhaust valve opening	164°CA
Exhaust valve closing	350°CA
Exhaust valve maximum lift	9,25 mm
Maximum torque	230 Nm at 1750 rpm
Maximum Power	68 kW at 4000 rpm

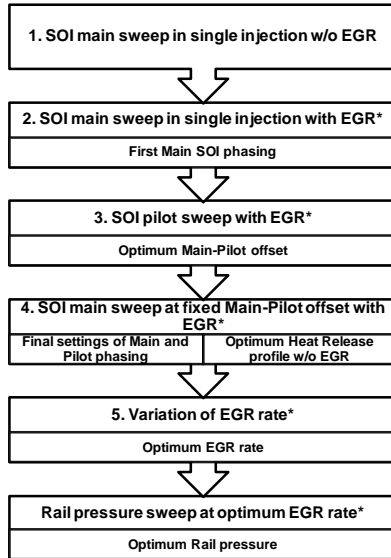
The experiment was conducted in double injection mode (i.e. pilot and main injection) with EGR. To cope with the high dispersion of fuels properties, particularly volatility and reactivity, the engine settings were adapted for each fuel. Matrix fuels were optimized separately on six operating points ranging from 1350 to 2400 rpm engine speed and from 1 to 13.4 bar of Brake Mean Effective Pressure (BMEP). These operating points are representative of the New European Driving Cycle (NEDC) and have been used to evaluate new formulation or engine concepts for reduced pollutants emissions by other groups [32], [9]. To better illustrate the main results, we present in this article two engine operating points selected in the light and middle load; 1500 rpm - 6 bar (EP1) and 2280 rpm – 8.2 bar (EP2). Both engine operating points are optimized using the same methodology for each fuel, allowing the definition successively of the optimum settings of main and pilot injections phasing, pilot quantity, EGR rate and rail pressure. The intake pressure was fixed to PSA’s standard calibration matching the maximum engine capacity. Pilot quantity was fixed to 1.5mg/stroke, corresponding to the average pilot quantity used in the stock calibration. To reduce the optimization time, the fuels were categorized into three cetane ranges (Group 1: 47-52, Group 2: 41-46 and Group 3: 35-40). Within each range, a “central” fuel was defined: Fuel 4, Fuel 7 and Fuel 11, respectively. Central fuels were optimized with a detailed method consisting of successive single parametric variations of main and pilot injection phasing, rail pressure and EGR rate. The optimum parameters are defined to achieve targets of NO_x, PM, noise, CO, HC and IMEP stability (summarized in Table 3) compliant with levels obtained in Euro 5-6 regulations, using similar test equipment [9]. The final optimized heat release profile was used as a baseline for the optimization of the fuels belonging to the same cetane group. An overview of both methodologies is provided in Figure 4. Note that the injection pressure was optimized for each fuel separately. The initial rail pressure for the “central” fuels (used in the optimization methodology) was that of the standard map, i.e. 800 bar for EP1 and 1146 bar for EP2, while, for the fuels belonging to the same cetane group, the initial rail pressure corresponds to the optimized pressure of the “central” fuel. It should be noted that fixed engine settings such as the intake pressure correspond to diesel like-fuels, and may influence the results of high volatility and low-cetane number fuels. For example, a higher intake may better highlight the potential of high volatility and low-cetane

number fuels according to previous work of Han et al. [17]. Further details on the optimization methodology are provided in Appendix B.

Table 3: Engine optimization criteria at 1500 rpm – 6 bar (EP1) and 2280 rpm – 8.2 bar (EP 2). () Fuel consumption is minimized if the pollutant targets are respected*

Parameter	Unit	Precision	Fixed settings and optimization criteria	
Engine speed	rpm	+/- 3	1500	2280
Engine load	bar	+/- 0.1	6	8.2
Intake pressure	bar	+/- 0.015	1.03	1.46
NOx	g/kWh	+/- 0.03	Minimize	Minimize
Particles	g/kWh	+/- 0.03	< 0.15	<0.2
CO	g/kWh	+/-1	< 8	<4
HC	g/kWh	+/-0.1	< 0.8	<0.4
COV	%	+/- 0.5	3	3
Noise	dB	+/- 1	85	89

Multiple sweep methodology



Heat release methodology

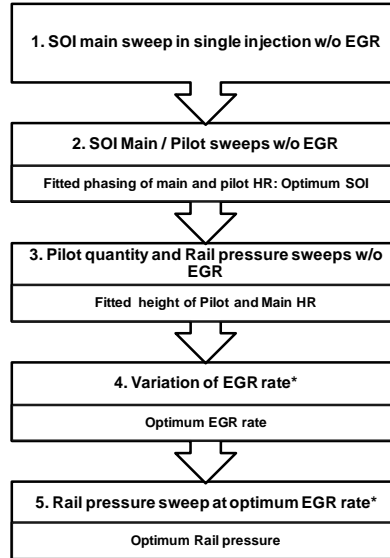


Figure 4: Overview of the optimization methodologies () optimum levels were determined in agreement with the target and constraints described in Table 3*

2.4 NO_x - PM tradeoff characterization

To characterize the NO_x-PM tradeoff, a quantified evaluation developed. Based on the NO_x and PM emissions measured during the final EGR sweep, exponential curves representing PM emissions as a function of NO_x (Figure 5) were fitted according to the following equation: $PM(g/kWh) = A(i,j) \exp(B(i,j)/NO_x(g/kWh))$, where A and B are fitting coefficients determined for the fuel i and operation point j. The correlation coefficients are above 0.95 for all matrix fuels optimized at different speed-load conditions. The integral of the curves (C_{PM}), calculated over a determined NO_x range, allowed the characterization of the NO_x-PM tradeoff. Fuels having a better NO_x-PM tradeoff would have a lower level of PM integral (or cumulated particulates) over the integration domain. The robustness of this evaluation was checked through a variation of the integration limits. This method for NO_x-PM tradeoff characterization aims to complete the more conventional optimum selection and point-to-point comparison. The latter may not be representative of the overall fuel behavior and may not be indicative of a fuel's sensitivity to small variation in engine settings, especially intake O₂ concentration. This method is usually poorly discriminating in the case of small differences.

3 Results

3.1 Fuel matrix evaluation

This section presents the results of the fuel matrix evaluation. To highlight the main fuel effect observed, only matrix fuels composed of binary mixtures with a significant percentage of light gasoline and kerosene streams are presented. Namely, Fuels 2, a diesel/kerosene blend and Fuels 5, 6, 10 and 12, which are gasoline/diesel blends. Fuel 4 composed of 100% HSRD was the reference fuel. Fuels are compared on engine conditions EP1 and EP2. Figure 5 illustrates the comparison of the NO_x-PM tradeoff and cumulated particulates (C_{PM}) over the NO_x optimum range, i.e. from 0.7 to 1.5 g/kW.h and from 1 to 2 g/kW.h on EP1 and EP2, respectively (Appendix C). To evaluate the robustness of this approach, the limits of the NO_x range were varied by +/- 0.5 g/kW.h, and results show negligible variation of the main

trends discussed hereafter. Moreover, optimum results summarized in Figure 6 are discussed to illustrate the variation of fuel consumption and other regulated pollutants with respect to streams composition. Engine results synthesis using the entire fuel matrix is summarized in Appendix C.

Effect of the addition of Hydrotreated Straight Run Gasoline (HSRG) to Diesel

On EP1, the addition of 50% HSRG to both diesel streams (HSRD or HCKLD, in Fuel 6 and Fuel 5, respectively) allows over 5 times lower C_{PM} compared with reference diesel Fuel 4. Through the combination of fuel's higher volatility and increased ignition delay, HSRG addition shifts the combustion towards the lower temperature range, thus reducing the NO_x emissions. The decrease of PM emissions may be associated with the fuel composition through lower fractions of aromatics and soot precursors especially in Fuel 5, in agreement with the results of Weall et al. investigating gasoline-diesel blends [30]. Similar conclusions were obtained by Han et al. [17], [16] showing that the addition of gasoline up to 40%vol allowed the simultaneous reduction of NO_x and soot emissions. Optimum results comparison (Figure 6) shows a reduction in fuel consumption and HC emissions (5% and 25%, respectively). However, carbon monoxide increased by 30% and 85%, for Fuel 5 and Fuel 6, respectively compared with Fuel 4. Lower fuel consumption can be associated with the shorter combustion duration (CA₉₀-CA₁₀ is half of that of diesel fuel), while the CO increase is mainly due to lower combustion efficiency typical of low cetane number fuels especially at high EGR rates [33], usually due to over-mixing leading to fuel-lean regions acting as carbon monoxide sources [14]. At the higher engine load of EP2, Fuels 5 and 6 present similar trends and NO_x-PM tradeoff is comparable to Fuel 4.

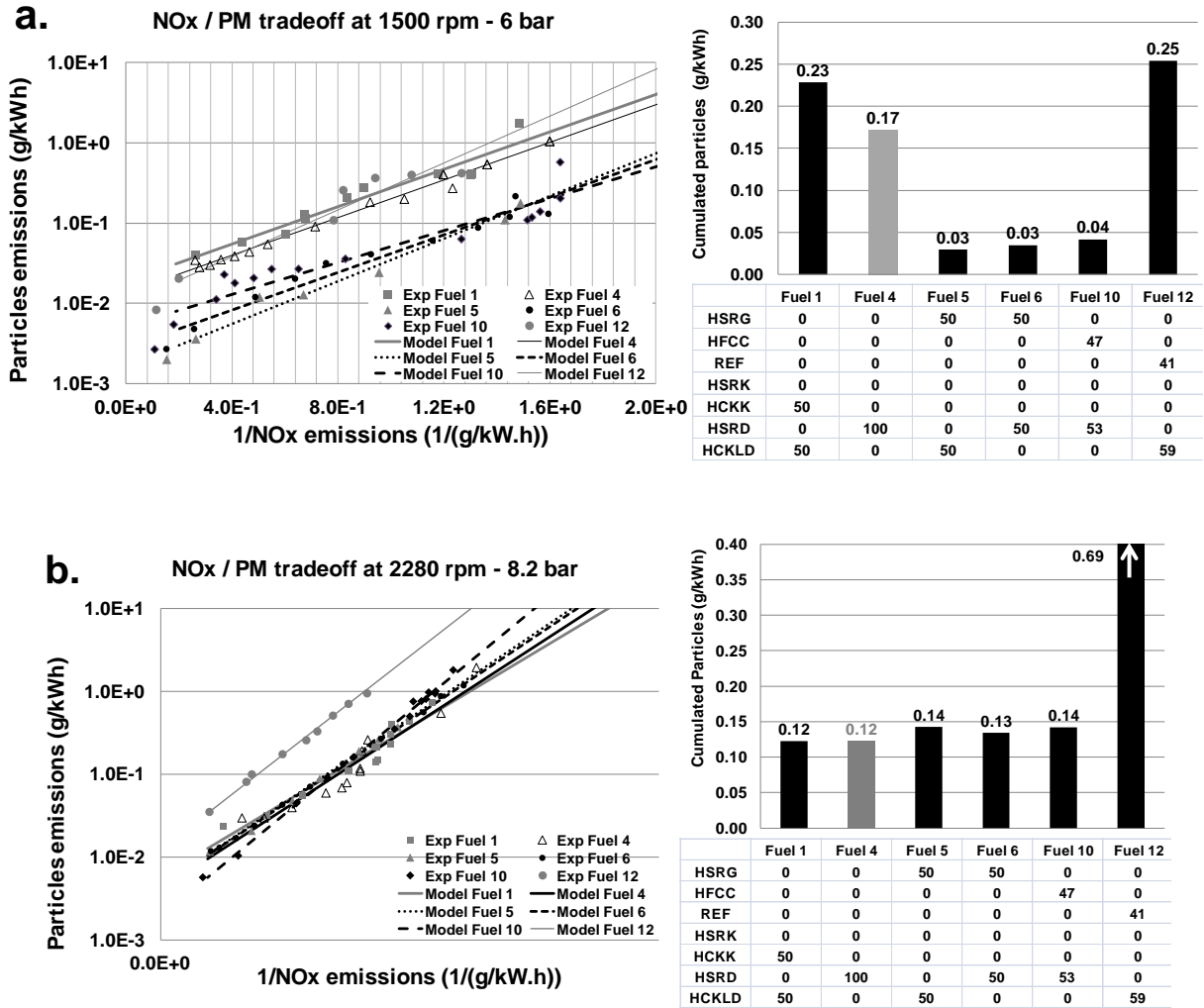


Figure 5: NOx-PM tradeoff during EGR sweeps (experiment and model) for several matrix fuels, CPM calculation a) EP1: 1500 rpm-6bar. b) EP2: 2280rpm-8.2 bar

This result is closely related to fuel characteristics. Later SOI, applied for diesel fuel allows for shifting the combustion towards the lower temperature range, whereas, the EGR rate is limited by the soot constraint. In the case of gasoline/diesel blends (Fuels 5 and 6), SOI is limited by stability, NOx emissions are lowered through the higher EGR rate possible by virtue of their low sooting tendency. Both strategies lead to a similar NOx-PM tradeoff, however, Fuels 5 and 6 present the advantage of reduced fuel consumption, through better combustion phasing and shorter combustion duration favored by better air fuel mixing.

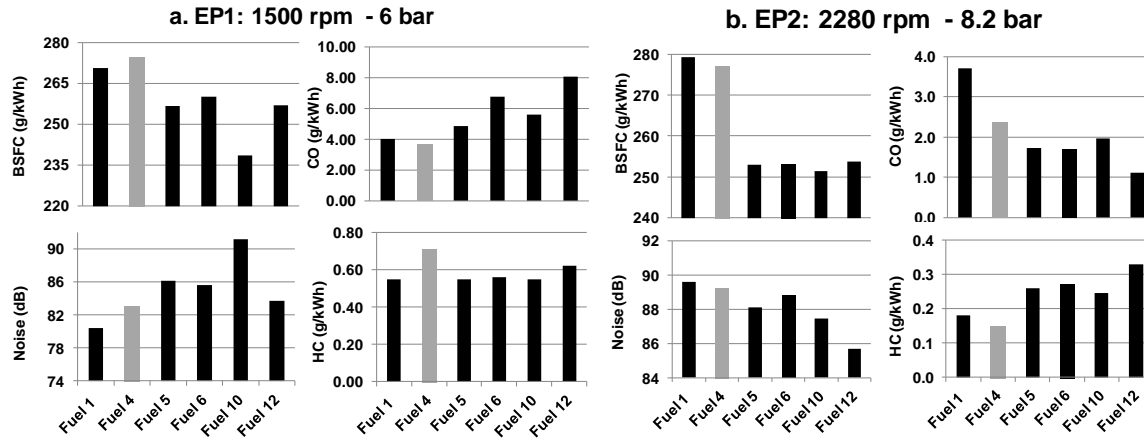


Figure 6: Optimized engine outputs of several matrix fuels tested at two engine conditions: a) EP 1: 1500 rpm-6bar and b) EP2: 2280rpm-8.2 bar

Effect of the addition of Hydrotreated Fluid Catalytic Cracking (HFCC) to Diesel

HFCC addition to HSRD studied in Fuel 10 reduces by over 4 times C_{PM} compared with HSRD. Low CN contributes to increase the autoignition delay, shifting the combustion towards lower temperatures which reduces NOx emissions. Additionally, the high volatility reduces the formation fuel rich areas and high olefin content ensures a high reaction rate [34] thus reducing PM emissions. Both effects allow for achieving very good NOx-PM tradeoff at EP1. Optimum results at EP1 (Figure 6), illustrate 13% lower fuel consumption and 23% lower HC emissions compared with Fuel 4. In fact, the higher rate of combustion of the olefin-rich HFCC stream reduces the combustion duration and favors thermal efficiency. CO emissions increase by over 45% comparably with the HSRG effect (Fuel 6). We note that noise level was very high (91 dB) and could not be reduced with the settings variation, most likely due to the increased autoignition delay and mixture-controlled combustion. At higher load at EP2, Fuel 10 presents roughly similar results to Fuel 4 in terms of NOx-PM tradeoff, CO, HC and noise. However, a better fuel economy is achieved mainly due to better phasing and shorter combustion promoted by better mixing.

Effect of the addition of Reformate (REF) to Diesel

The addition of around 40% REF to HCKLD in Fuel 12 leads to a significant degradation in the C_{PM} performance (8 times higher than the HSRG/HCKLD mixture and 50% higher than reference diesel). This trend can be attributed to the low CN of Fuel 12 and the low combustion stability that limits EGR capacity. Both contribute to NO_x formation through increased mixture-controlled high temperature combustion, thus, confirming a negative effect of excessive ignition delay on exhaust emissions observed by other groups [35]. Moreover, the higher aromatic fraction provided by the REF stream contributes to an increase in the soot precursors and can also play a role in increasing NO_x formation [24]. Contrary to the HSRG and HFCC effect on NO_x-PM, which drops off at higher load, the negative effect of REF addition to diesel is more pronounced at higher load (Figure 5). A fair linear relationship between C_{PM} and REF volume fraction is obtained. Optimum results show a similar positive trend on fuel consumption on EP1 and EP2 and CO emissions increase on EP1 in agreement with the other gasoline streams.

Effect of the addition of Hydrocracked Kerosene (HCKK) to Diesel

The addition of HCKK kerosene stream to HCKLD in Fuel 1 leads to an increase in C_{PM} by over 7 times compared with HSRG in the same proportion (Fuel 5) at EP1. Its lower volatility and higher cetane number reduces the mixing efficiency and favors the formation of fuel-rich areas which increases the sooting tendency. The fuel chemistry can also contribute to a NO_x rise through lower paraffin and higher naphthenes fractions. The NO_x relationship to the molecular structure of alkanes studied in literature shows higher NO_x tendency for cyclic paraffins compared to normal and branched ones [24][36]. At higher load, the addition of HCKK has a relatively small impact on NO_x-PM tradeoff. Optimum results presented in Figure 6 illustrate higher fuel consumption at EP1 and EP2, and reduced CO emissions at EP1 which confirms the previous hypothesis. Overall, we observe that kerosene/diesel blends behave similarly to diesel streams in terms of engine efficiency and regulated pollutants.

Summary

The analysis of engine results allows a first evaluation of both the direct and synergistic effects of refinery streams on engine outputs. The results suggest a significant impact of gasoline streams composition on the NO_x/PM/fuel economy trade off. REF addition to diesel streams appears to degrade the NO_x-PM tradeoff at both engine loads. HSRG illustrates a good potential for simultaneously reducing NO_x, PM and fuel consumption with an acceptable increase of carbon monoxide at light load. The addition of olefins-rich HFCC to HSRD diesel streams is also favorable for NO_x / PM trade-off at light load. Finally, the HCKK stream shows diesel-like behavior at light and high load, with rather degraded CO emissions. Results show a sensitivity of the NO_x-PM tradeoff to streams composition which varies with the engine load: lower load engine conditions, characterized by higher homogeneity, are more sensitive to the fuel properties than higher load conditions.

3.2 Modeling of engine outputs and optimization function of the refinery streams composition

Linear models with no interaction were built linking optimum results obtained at EP1 and EP2 to the refinery streams' volume fractions. Figure 7 presents predicted and experimental results for several engine outputs of matrix fuels (Fuels 1-12) along with the validation fuel (Fuel 13). Results are normalized from 0 to 1 at the scale of all the experimental results. Details of the model coefficients and statistical data are summarized in Appendix D.

Fuel consumption has a determination coefficient (R^2) above 0.97 for both EP 1 and EP2; Results of Fuel 13 overestimate fuel consumption by 8% for EP1 and are fairly predictive for EP2. NO_x and PM models have low determination coefficients (0.78 and 0.62 respectively for EP1 and 0.93 and 0.45, respectively for EP2). The poor performance of the PM model at EP2 can be associated with the quasi-equity of particulate emissions at the optimum point for most fuels (Appendix C). The models accurately predict EP2 NO_x level for Fuel 13 and within twice the standard deviation interval (σ) for EP1. PM emissions are

within twice (σ) at both operating points. The quality of the CO and HC emissions models was good for EP2 and fair for EP1 (Appendix D). Fuel 13 results were fairly predicted for both. Finally, the model of C_{PM} was fair on EP1 ($R^2=0.65$) and good on EP2 ($R^2=0.93$). The prediction of Fuel 13 level was fair only for EP2 and poor for EP1.

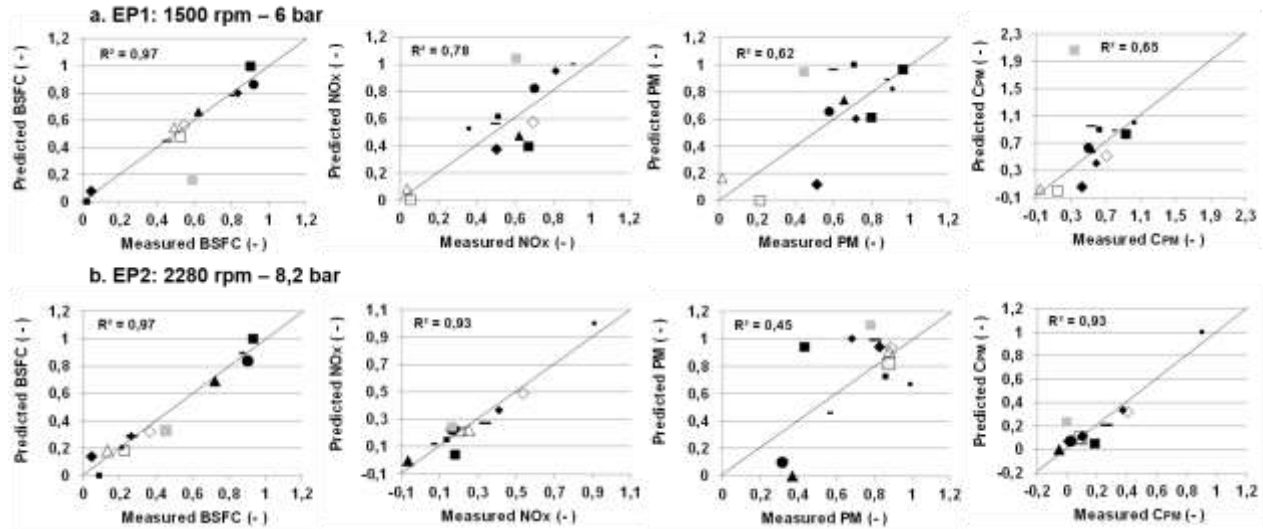


Figure 7: Modeling of the engine outputs based on optimum results at EP1 (1500rpm – 6 bar) and EP2 (2280 rpm-8.2 bar). Symbols: (-): Fuel 1, (♦): Fuel 2, (■): Fuel 3, (●): Fuel 4, (□): Fuel 5, (Δ): Fuel 6, (—): Fuel 7, (▲) Fuel 8, (◇): Fuel 9, (◆): Fuel 10, (▣): Fuel 11, (●): Fuel 12 and (Gray ■) Fuel 13.

Figure 8 presents the normalized correlation coefficients. They illustrate the contribution of the different refinery streams to fuel consumption, NOx and particulates on EP1 and EP2. **Fuel consumption coefficients** are similar for EP1 and EP2 where diesel and kerosene streams have higher coefficients compared with gasoline streams and in agreement with the previous analysis. At light load, HSRG and HFCC streams reduces heat rejection through lower combustion temperature, while at mid load, they induce later and higher temperature premixed combustion, thus increasing the combustion efficiency (Figure 6). **NOx coefficients** vary significantly between EP1 and EP2. EP 1 presents a higher sensitivity to

streams composition. The lowest coefficients are associated with HSRG and REF, then HFCC, while diesel and kerosene streams are more similar, confirming previous conclusions. At higher load, HFCC and HSRG streams' coefficients become higher than both kerosene and diesel, although of a similar magnitude. REF has the worst effect on NO_x emissions, three times higher than standard diesel and over twice as high as the other gasoline streams. **PM coefficients** are lower for gasoline streams HSRG and HFCC at light load and tend to increase at mid load. Only REF presented high PM coefficients for both EP1 and EP2. HSRD and kerosene streams present a good tradeoff with average levels at EP1 and EP2. The **coefficients of the C_{PM}** model, in agreement with the previous analysis of NO_x and PM coefficients, underline the negative effect of REF stream on EP1 and more significantly on EP2, and the suitability of gasoline streams HSRG and HFCC at light load with low coefficients and kerosene and diesel streams at mid load.

To summarize, modeling of the engine outputs allows qualitative representation of the main streams effects described in section 2.1. The models' accuracy was fair for several engine outputs over the tested conditions, however not sufficiently predictive for the results of the validation fuel. This may be associated to the relatively low number of fuels used to build the model. Besides, the model did not take into account streams' interactions, that may have an influence as well. Therefore, two approaches were evaluated, for fuel optimization, first, through the minimization of pollutants (NO_x and PM trade off), then through a comparative evaluation of the optimized fuel with matrix fuels.

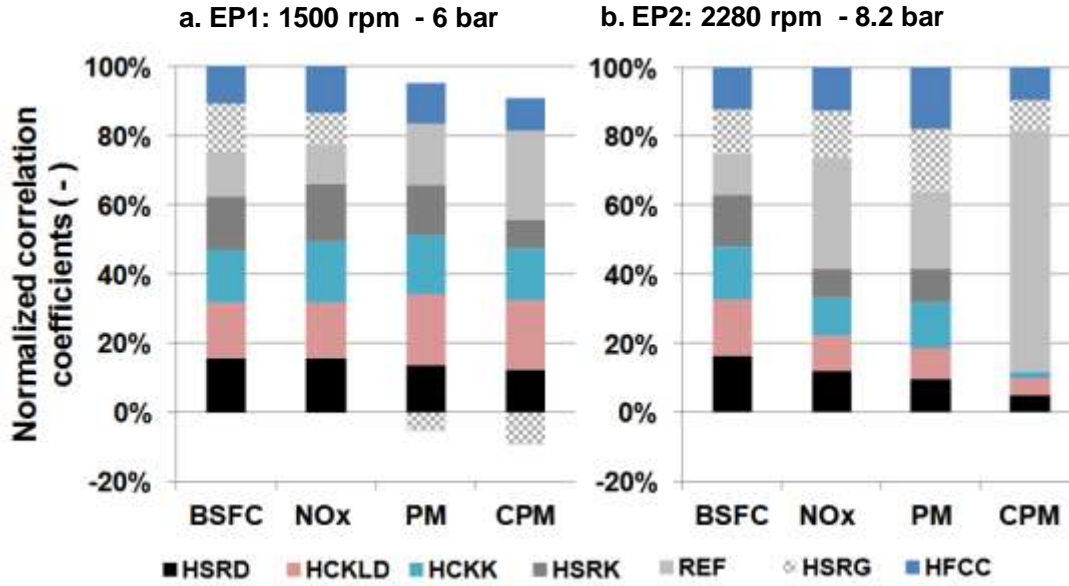


Figure 8: Normalized correlation coefficient of the linear model for a. EP 1 and b. EP 2 function of the volume fraction of the refinery streams

Based on the developed models, an optimization was carried out, aimed at proposing a streams composition allowing for the best NOx-PM tradeoff through the minimization of C_{PM} criterion averaged on EP1 and EP2 $C_{PM} = \frac{C_{PM}(EP1) + C_{PM}(EP2)}{2}$. The optimization was carried out under the same constraints on EP1 and EP2 for PM, CO, HC and stability adopted for the matrix fuel evaluation methodology (Table 3). Interestingly, the optimum composition is one of the matrix fuels tested: Fuel 6, a diesel/gasoline blend composed of 50%v HSRD and 50%v HSRG, in good agreement with the ranking of the fuels according to average C_{PM} displayed in Figure 9. This fuel allows, at light load, a drastic reduction in NOx emissions and a low sooting tendency, and a fairly good behavior at mid load.

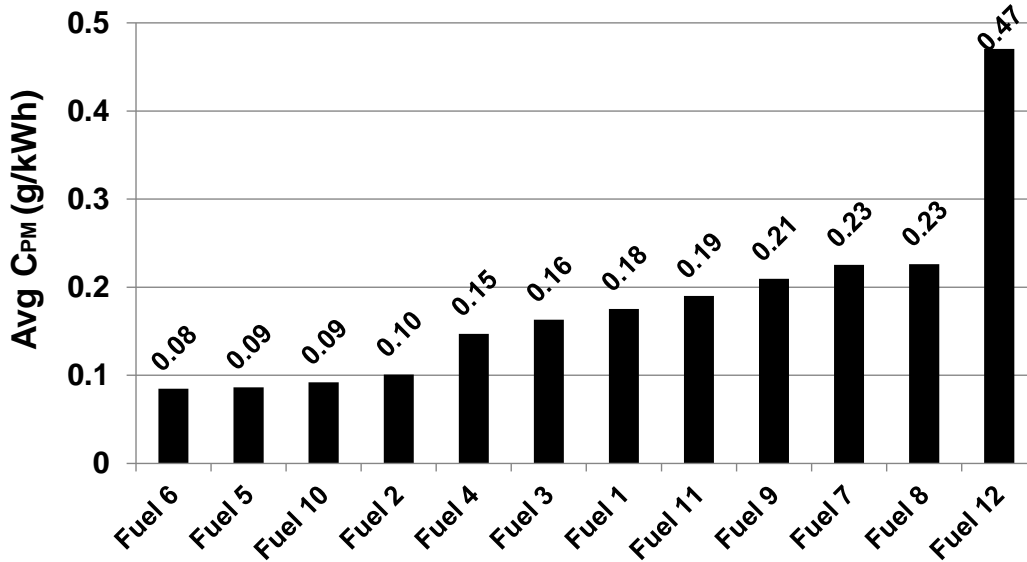


Figure 9: Ranking of the fuel matrix according to NO_x-PM Tradeoff: Average of C_{PM} on EP1 and EP2

4 Conclusions

In this study, we propose an original methodology to optimize the fuel formulation for compression ignition light-duty engines, to achieve lower pollutants emissions and higher engine efficiency based on a DoE approach. Seven refinery streams representative of gasoline, kerosene and diesel cuts are used. A D-Optimal mixture design was applied to build, a 12-run, 7-factor fuel matrix. Fuels were thoroughly optimized on light and mid load engine points representative of typical vehicle running conditions. The results show a high sensitivity of the engine efficiency and pollutants emissions to streams composition. Optimal fuel requirements varied as a function of the engine operating point. At light load, the addition of up to 50% gasoline streams (mainly HSRG) to diesel streams demonstrates a better potential to achieve simultaneously low NO_x and PM emissions and an overall good engine performance. Reformate, a highly aromatic gasoline stream, did not offer an advantage at any of the tested conditions due to high particulate emissions. The two kerosene streams evaluated in this work performed similarly to diesel streams in terms of engine efficiency and pollutants emissions. A compromise fuel is proposed composed of 50%vHSRG

412 and 50%vHSRD that allows halving of NO_x and PM emissions and reducing of fuel consumption by
413 5%wt compared to reference diesel HSRD.

414 This study allowed to put forward an interesting potential of using gasoline and kerosene streams in diesel
415 fuels on a commercial light-duty diesel engine (PSA DV6D). The optimization methodology was based on
416 reduced number of parameters and interactions. A more elaborated engine calibration would be necessary
417 to confirm the observed trends on larger range of operating conditions. Besides, the upgrading of the
418 engine hardware (especially, in terms of boost pressure and combustion chamber design) may allow to
419 further explore the full potential of these streams in terms of engine performance and emissions.

420 **5 Acknowledgement**

421 Authors acknowledge the valuable support of Saudi Aramco to this research work and would like to thank
422 Romain CHERBLAND and Yoan LEMONNIER from IFP Energies Nouvelles for conducting the engine
423 experiments and Frederic NICOLAS from IFP Energies Nouvelles for engine calibration support.

6 References

- [1] “EU Transport in Figures - Statistical Pocketbook 2014,” European Commission, Tech. Rep., 2014.
- [2] A. Capros, N. Devitan, and T. D. et al, “EU Energy, Transport and GHG emissions Trends to 2050, Reference scenario 2013,” European commission, Tech. Rep., 2013.
- [3] R. H. Stanglmaier and C. E. Roberts, “Homogeneous charge compression ignition (HCCI): benefits, compromises, and future engine applications,” SAE Technical Paper, Tech. Rep., 1999.
- [4] M. Christensen, A. Hultqvist, and B. Johansson, “Demonstrating the Multi Fuel Capability of a Homogeneous Charge Compression Ignition Engine with Variable Compression Ratio,” *SAE Technical Paper*, vol. 1999-01-3679, 1999.
- [5] L. Pesant and L. Forti, “IFP International consortium Effects of fuel and additives on diesel HCCI engines, 4th year, final report,” IFPEN, Tech. Rep., 2008.
- [6] M. Muether, M. Lamping, A. Kolbeck, R. F. Cracknell, D. J. Rikeard, and K. D. Rose, “Advanced Combustion for Low Emissions and High Efficiency Part 1: Impact of Engine Hardware on HCCI Combustion,” *SAE Technical Paper*, vol. 2008-01-2405, 2008.
- [7] C. Noehre, M. Andersson, B. Johansson, and A. Hultqvist, “Characterization of partially premixed combustion,” SAE Technical Paper, Tech. Rep., 2006.
- [8] G. T. Kalghatgi, P. Risberg, and H.-E. Angstrom, “Partially Pre-Mixed Auto-Ignition of Gasoline to Attain Low Smoke and Low NO_x at High Load in a Compression Ignition Engine and Comparison with a Diesel Fuel,” *SAE Technical Paper*, vol. 2007-01-0006, 2007.

- 444 [9] A. Warey, J.-P. Hardy, M. Hennequin, M. Tatur, D. Tomazic, and W. Cannella, "Fuel Effects on
445 Low Temperature Combustion in a Light-Duty Diesel Engine," *SAE Technical Paper*, vol. 2010-01-1122,
446 2010.
- 447 [10] T. Zannis and D. Hountalas, "Effect of fuel aromatic content and structure on direct-injection
448 diesel engine pollutant emissions," *Journal of the Energy Institute*, vol. 77, no. 511, pp. 16–25, 2004.
- 449 [11] R. F. Cracknell, D. J. Rikeard, J. Ariztegui, K. D. Rose, M. Muether, M. Lamping, and
450 A. Kolbeck, "Advanced Combustion for Low Emissions and High Efficiency Part 2: Impact of Fuel
451 Properties on HCCI Combustion," *SAE Technical Paper*, vol. 2008-01-2404, 2008.
- 452 [12] A. S. E. Cheng, B. T. Fisher, G. C. Martin, and C. J. Mueller, "Effects of Fuel Volatility on Early
453 Direct-Injection, Low-Temperature Combustion in an Optical Diesel Engine," *Energy & Fuels*, vol. 24,
454 no. 3, pp. 1538–1551, 2010. [Online]. Available: <http://pubs.acs.org/doi/abs/10.1021/ef9011142>
- 455 [13] P. Miles, "Sources and mitigation of CO and UHC emissions in low-temperature diesel
456 combustion regimes: Insights obtained via homogeneous reactor modeling," in *13th Diesel Engine
457 Efficiency and Emissions Research Conference, August 13-16, Detroit, Michigan, 2007*.
- 458 [14] M. P. Musculus, T. Lachaux, L. M. Pickett, and C. A. Idicheria, "End-of-injection over-mixing
459 and unburned hydrocarbon emissions in low-temperature-combustion diesel engines," *SAE Technical
460 Paper, Tech. Rep.*, 2007.
- 461 [15] S. M. Aceves, D. L. Flowers, C. K. Westbrook, J. R. Smith, W. Pitz, R. Dibble, M. Christensen,
462 and B. Johansson, "A multi-zone model for prediction of HCCI combustion and emissions," *SAE
463 Technical paper, Tech. Rep.*, 2000.
- 464 [16] D. Han, A. M. Ickes, S. V. Bohac, Z. Huang, and D. N. Assanis, "Premixed low-temperature
465 combustion of blends of diesel and gasoline in a high speed compression ignition engine," *Proceedings of*

466 *the Combustion Institute*, vol. 33, no. 2, pp. 3039 – 3046, 2011. [Online]. Available: [http://-](http://www.sciencedirect.com/science/article/pii/S1540748910003081)
467 www.sciencedirect.com/science/article/pii/S1540748910003081

468 [17] D. Han, A. M. Ickes, D. N. Assanis, Z. Huang, and S. V. Bohac, “Attainment and Load Extension
469 of High-Efficiency Premixed Low-Temperature Combustion with Dieseline in a Compression Ignition
470 Engine,” *Energy & Fuels*, vol. 24, no. 6, pp. 3517–3525, 2010. [Online]. Available: [http://pubs.acs.org/-](http://pubs.acs.org/doi/abs/10.1021/ef100269c)
471 [doi/abs/10.1021/ef100269c](http://pubs.acs.org/doi/abs/10.1021/ef100269c)

472 [18] P. Risberg, G. Kalghatgi, H.-E. Ångström, and F. Wåhlin, “Auto-ignition quality of diesel-like
473 fuels in HCCI engines,” SAE Technical Paper, Tech. Rep., 2005.

474 [19] P. Bergstrand, “Effects on combustion by using kerosene or MK1 diesel,” SAE Technical Paper,
475 Tech. Rep., 2007.

476 [20] A. P. Singh and A. K. Agarwal, “Dieseline, Diesohol and Diesosene Fuelled HCCI Engine
477 Development,” SAE Technical Paper, Tech. Rep., 2015.

478 [21] K. Nakakita, H. Ban, S. Takasu, Y. Hotta, K. Inagaki, W. Weissman, and J. T. Farrell, “Effect of
479 hydrocarbon molecular structure in diesel fuel on in-cylinder soot formation and exhaust emissions,” SAE
480 Technical Paper, Tech. Rep., 2003.

481 [22] J. Song and K. O. Lee, “Fuel Property Impacts on diesel particulate morphology, nanostructures,
482 and NO_x emissions,” SAE Technical Paper, Tech. Rep., 2007.

483 [23] Y. Takatori, Y. Mandokoro, K. Akihama, K. Nakakita, Y. Tsukasaki, S. Iguchi, L. I. Yeh, and
484 A. M. Dean, “Effect of Hydrocarbon Molecular Structure on Diesel Exhaust Emissions Part 2: Effect of
485 Branched and Ring Structures of Paraffins on Benzene and Soot Formation,” in *SAE Technical Paper*.
486 SAE International, 10 1998. [Online]. Available: <http://dx.doi.org/10.4271/982495>

- 487 [24] F. Bachmaier, K. Eberius, and T. Just, "The formation of nitric oxide and the detection of HCN in
488 premixed hydrocarbon-air flames at 1 atmosphere," *Combustion Science and Technology*, vol. 7, no. 2, pp.
489 77–84, 1973.
- 490 [25] S.-S. Kee, A. Mohammadi, Y. Kidoguchi, and K. Miwa, "Effects of Aromatic Hydrocarbons on
491 Fuel Decomposition and Oxidation Processes in Diesel Combustion," in *SAE Technical Paper*. SAE
492 International, 05 2005. [Online]. Available: <http://dx.doi.org/10.4271/2005-01-2086>
- 493 [26] M. Al-Abdullah, G. Kalghatgi, and H. Babiker, "Flash points and volatility characteristics of
494 gasoline/diesel blends," *Fuel*, vol. 153, pp. 67 – 69, 2015. [Online]. Available: [http://-](http://www.sciencedirect.com/science/article/pii/S0016236115002239)
495 www.sciencedirect.com/science/article/pii/S0016236115002239
- 496 [27] M. Castagne, Y. Bentolila, F. Chaudoye, H. A., F. Nicolas, and D. Sinoquet, "Comparison of
497 different calibration methods based on design of experiments," *Oil & Gas Science and Technology - Rev.*
498 *IFP*, vol. 63, no. 4, pp. 563–582, 2008. [Online]. Available: <http://dx.doi.org/10.2516/ogst:2008029>
- 499 [28] R. T. Butts, D. Foster, R. Krieger, M. Andrie, and Y. Ra, "Investigation of the Effects of Cetane
500 Number, Volatility, and Total Aromatic Content on Highly- Dilute Low Temperature Diesel
501 Combustion," *SAE Technical Paper*, vol. 2010-01-0337, 2010.
- 502 [29] M. J. Anderson, *Design-Expert Software V9 Tutorials*. Stat-Ease, Inc., 2014.
- 503 [30] A. Weall and N. Collings, "Investigation into Partially Premixed Combustion in a Light-Duty
504 Multi-Cylinder Diesel Engine Fuelled with a Mixture of Gasoline and Diesel," *SAE Technical Paper*, vol.
505 2007-01-4058, 2007.
- 506 [31] K. S. Pedersen, A. Fredenslund, P. L. Christensen, and P. Thomassen, "Viscosity of crude oils,"
507 *Chemical Engineering Science*, vol. 39, no. 6, pp. 1011 – 1016, 1984. [Online]. Available: [http://-](http://www.sciencedirect.com/science/article/pii/0009250984870098)
508 www.sciencedirect.com/science/article/pii/0009250984870098

- 509 [32] J. Chang, G. Kalghatgi, A. Amer, P. Adomeit, H. Rohs, and B. Heuser, "Vehicle Demonstration
510 of Naphtha Fuel Achieving Both High Efficiency and Drivability with EURO6 Engine-Out NO_x
511 Emission," *SAE International Journal of Engines*, vol. 6, no. 1, pp. 101–119, 2013.
- 512 [33] Y. Jeihouni, S. Pischinger, L. Ruhkamp, and T. Koerfer, "Relationship between fuel properties
513 and sensitivity analysis of non-aromatic and aromatic fuels used in a single cylinder heavy duty diesel
514 engine," SAE Technical Paper, Tech. Rep., 2011.
- 515 [34] L. Starck, B. Lecointe, L. Forti, and N. Jeuland, "Impact of fuel characteristics on {HCCI}
516 combustion: Performances and emissions," *Fuel*, vol. 89, no. 10, pp. 3069 – 3077, 2010. [Online].
517 Available: <http://www.sciencedirect.com/science/article/pii/S001623611000253X>
- 518 [35] K. Kitano, R. Nishiumi, Y. Tsukasaki, T. Tanaka, and M. Morinaga, "Effects of Fuel Properties
519 on Premixed Charge Compression Ignition Combustion in a Direct Injection Diesel Engine," *SAE*
520 *Technical Papers*, vol. 2003-01-1815, 05 2003. [Online]. Available: [http://dx.doi.org/10.4271/2003-01-](http://dx.doi.org/10.4271/2003-01-1815)
521 1815
- 522 [36] L. J.C.Y. and M. P.C., "NO_x as a function of fuel for C₁-to-C₁₆ hydrocarbons and methanol
523 burned in a high intensity, lean-premixed, combustion reactor." in *WSS Meeting, Combustion Institute*,
524 1998.
- 525 [37] R. Lugo, V. Ebrahimian, C. Lefebvre, and C. e. a. Habchi, "A Compositional Representative Fuel
526 Model for Biofuels - Application to Diesel Engine Modelling," *SAE Technical Paper*, vol. 2010-01-2183,
527 2010.

528 7 Appendices

529 *Appendix A: Main properties of the studied refinery streams*

Analyses	Method	Unit	REF	HFCC	HSRG	HCKK	HSRK	HCKLD	HSRD
Density at 15°C	ASTM D4052	kg/m3	868.4	691.9	741.1	812.2	787.7	818.7	836.6
Viscosity 40°C	EN ISO 3104	mm²/s	0.5958	0.36	0.5685	1.342	1.122	2.634	3.297
LHV	ASTM D240	MJ/kg	41.03	44.46	44.29	43.89	40.73	43.57	42.57
Sulfur	NF EN ISO 20846	mg/kg	<0.5	5.7	<0.5	<0.5	221	<0.5	1.5
CN (CFR)	ASTM D613	-	6.1*	16.5*	34.8	45.4	49.0	54.9	51.3
H/C/N (IFPEN)	CG								
C		% wt	90.5	85.9	85.4	86.0	85.8	85.8	86.4
H		% wt	9.5	14.1	14.6	13.8	14.1	14.0	13.6
N		% wt					0.09	0.12	
O		% wt				0.11		0.11	
Total		% wt	100.0	100.0	100.0	100.0	100.0	100.0	100.0
H/C		-	1.255	1.970	2.056	1.930	1.971	1.958	1.889
Composition	GCxGC		8535	8533	8534	8532	8531	8536	8537
Paraffins		% wt	2.15	33.1	59.0	36.3	57.2	43.4	29.9
Naphthenes		% wt	0.14	7.0	27	43	18.5	40.2	25
Olefins		% wt	0.17	45.0	0	0	0	0	0
Aromatics		% wt	97.5	14.8	13.9	20.7	24.3	16.4	45.3
Monoaromatics		% wt	96.7	14.8	13.9	19.5	23.3	14.7	41.7
Polyaromatics		% wt	0.8	0.0	0.0	1.2	1	1.7	3.6
Distillation	EN ISO 3405								
0		°C	105.8	30.4	81	166.9	149.9	123.9	187.9
5		°C	119.5	36.9	98	184.6	165.8	207.4	201.3
10		°C	121.5	39	102.1	190.4	169.7	229.8	206.7
15			122.9	40.3	104.9	193.4	173	241.1	213.4
20		°C	124.1	41.4	107.6	196.2	175.6	247.6	220.8
30		°C	126.2	43.7	112.4	200.7	181.1	257.7	240.6
40		°C	128.7	46.3	117	204.3	186.2	264.9	268.5
50		°C	131.6	49.6	122.9	207.5	191.5	271.7	296.7
60		°C	135.1	54.1	129.1	210.9	197.5	278.5	320.1
70		°C	140.2	61.1	135	214.5	205.4	284.7	344.7
80		°C	146.8	72.8	143	219.4	215.9	292.5	362.7
90		°C	156.7	88.9	152.7	226.4	231.6	304	373.6
95		°C	166.9	98.8	160.1	232	244.8	312.4	378.8
100		°C	198.7	115.4	171.2	243.4	267.8	320.2	381
Recovery at 250°C		% v/v				>98	96.3	22.6	33.9

Recovery at 350°C		% v/v				>98	>98	>98	72.3
Residue		% v/v	1.2	0.7	0.9				

* The Cetane Number (CN) of the streams is measured using a CFR engine, with 2 or 3 repeatability tests except for REF and HFCC that presented a very low reactivity. Their cetane number was evaluated through blending methods with higher CN streams (namely, HSRK, HSRD, HCKLD and HCKK).

Viscosity is measured using the standard test method (EN ISO 3104) at 40°C except HFCC (due to high volatility; IBP=30°C). The viscosity of HFCC is calculated using thermodynamic Pedersen model [37].

Appendix B: Engine optimization methodology and targets

In this section, the detailed and simplified method for fuels optimization are evaluated on the same Fuel in order to quantify the sensitivity to the fuels classification into cetane groups of the engine results. Fuel 5 having a central cetane number of 46.1 is tested using multiple sweeps method, and Iso-heat release method in Group 1 and Group 2 (i.e. through the imitation of optimum heat release of Fuel 4 and Fuel 7, respectively) at 3 different engine conditions. The comparison of optimum results shows almost 10% variation of BSFC on average. The amplitude of NOx and PM variation according to the optimization methodology is on average 0.14 and 0.03 g/kW.h, respectively. Optimization methodology impacts mostly the noise level due to its tight relationship with the injection settings. As an initial evaluation of the approach, the sensitivity of engine results to the methodology is taken into account as if it were an engine measurement dispersion error.

EP 1 : 1500 rpm - 6 bar									
Fuel reference	BSFC (g/kWh)	NOx (g/kWh)	PM (g/kWh)	CO (g/kWh)	HC (g/kWh)	CO2 (g/kWh)	noise dB	stab %	C PM g/kWh
Fuel 1	271	1.48	0.12	4.00	0.55	848	80	0.85	0.228
Fuel 2	271	1.46	0.09	3.80	0.49	849	83	0.78	0.121
Fuel 3	281	1.22	0.12	7.10	0.59	878	82	0.96	0.217
Fuel 4	274	1.40	0.09	3.65	0.71	860	83	1.90	0.171
Fuel 5	257	1.05	0.02	4.86	0.55	799	86	0.82	0.030
Fuel 6	260	1.08	0.04	6.74	0.56	806	86	0.93	0.035
Fuel 7	255	1.29	0.12	4.29	0.64	802	83	1.21	0.242
Fuel 8	265	1.25	0.10	6.04	0.64	834	82	1.04	0.169
Fuel 9	261	1.29	0.09	5.07	0.50	824	83	2.14	0.143
Fuel 10	238	1.21	0.04	5.61	0.55	742	91	0.94	0.042
Fuel 11	235	1.31	0.13	4.22	0.58	733	89	1.09	0.231
Fuel 12	257	1.27	0.11	8.07	0.62	814	84	1.15	0.254
Fuel 13	242	1.50	0.12	1.39	0.26	761	85	1.09	0.492

549

EP 2 : 2280 rpm - 8.2 bar									
Fuel reference	BSFC (g/kWh)	NOx (g/kWh)	PM (g/kWh)	CO (g/kWh)	HC (g/kWh)	CO2 (g/kWh)	noise dB	stab %	C PM g/kWh
Fuel 1	279	1.15	0.15	3.72	0.18	876	90	0.69	0.123
Fuel 2	272	1.02	0.10	3.10	0.18	852	91	0.68	0.081
Fuel 3	283	1.06	0.20	4.05	0.17	891	89	0.74	0.109
Fuel 4	277	1.25	0.11	2.37	0.15	872	89	0.67	0.123
Fuel 5	253	1.26	0.19	1.73	0.26	792	88	0.69	0.143
Fuel 6	253	1.25	0.20	1.68	0.27	793	89	1.08	0.135
Fuel 7	257	1.30	0.21	1.57	0.30	811	88	0.65	0.209
Fuel 8	257	1.39	0.21	2.09	0.28	815	90	0.90	0.284
Fuel 9	258	1.52	0.20	1.30	0.24	822	88	0.90	0.276
Fuel 10	251	1.24	0.20	1.96	0.25	790	87	0.74	0.142
Fuel 11	246	1.18	0.18	1.62	0.20	774	88	1.17	0.149
Fuel 12	254	2.04	0.17	1.12	0.33	816	86	0.60	0.687
Fuel 13	258	1.27	0.22	1.79	0.20	812	87	0.62	0.223

550

Appendix D: Synthesis of the models data of main engine outputs. Modeling was made on optimum results of EP1 (1500rpm – 6 bar) and EP2 (2280 rpm-8.2 bar): Correlation coefficients, standard deviations and determination coefficients

Refinery stream	EP 1: 1500 rpm - 6 bar						
	BSFC	NOx	PM	CO	HC	Noise	Stability
	g/kWh	g/kWh	g/kWh	g/kWh	g/kWh	dB	%
HSRG	238	0.77	-0.03	6.41	0.48	89	0.46
HFCC	192	1.17	0.07	4.52	0.50	98	0.73
REF	228	0.96	0.11	12.71	0.68	85	1.95
HSRK	269	1.44	0.09	2.98	0.51	81	0.49
HCKK	263	1.50	0.10	2.23	0.43	80	1.66
HSRD	277	1.35	0.08	4.72	0.68	83	1.74
HCKLD	280	1.37	0.12	5.25	0.60	82	0.87
std dev	3.24	0.09	0.03	1.28	0.06	1.25	0.36
R ²	0.97	0.78	0.62	0.64	0.54	0.93	0.68

Refinery stream	EP 2: 2280 rpm - 8.2 bar						
	BSFC	NOx	PM	CO	HC	Noise	Stability
	g/kWh	g/kWh	g/kWh	g/kWh	g/kWh	dB	%
HSRG	223	1.4	0.3	-0.1	0.4	88	1.1
HFCC	213	1.3	0.3	-0.1	0.3	86	1.2
REF	207	3.3	0.3	-3.0	0.6	81	0.8
HSRK	262	0.9	0.1	2.9	0.2	93	0.9
HCKK	269	1.1	0.2	2.7	0.2	90	0.9
HSRD	279	1.2	0.1	2.8	0.2	89	0.7
HCKLD	286	1.0	0.1	4.1	0.1	89	0.6
std dev	3.03	0.10	0.04	0.55	0.03	0.33	0.22
R ²	0.97	0.93	0.45	0.84	0.90	0.97	0.31